Technical Note

Frequency-Based Crack Effect Study on Beams Under Free Vibration Using Finite Element Analysis

Ompriya SAHU[1)], Priyadarshi DAS[1),*], Manoj Kumar MUNI[2)],
Nibedita PRADHAN[1)], Bidyadhar BASA[1)], Shishir Kumar SAHU[3)]

[1)] *Department of Civil Engineering, Institute of Technical Education and Research,*
Siksha 'O' Anusandhan University
Bhubaneswar, Odisha, India

[2)] *Department of Mechanical Engineering, Indira Gandhi Institute of Technology*
Sarang, Dhenkanal, Odisha, India

[3)] *Department of Civil Engineering, National Institute of Technology Rourkela*
Odisha, India

*Corresponding Author e-mail: priyadarshidas@soa.ac.in

A numerical computation-based analysis of the free vibration analysis of uniform beams with rectangular cross-sections is presented in this work using finite element analysis. The approach involves dividing the beam into segments at the crack section, which is then modelled for simulation for eigenfrequencies on the ABAQUS platform. The numerical simulation results are in excellent agreement with the findings of previous research, confirming the efficacy and applicability of the developed beam model. A sequential comprehensive approach towards analysis of the effects of the position and depth of the cracks on the natural frequencies are addressed in numerical results. The research findings confirm that the simulation model is suitable for the vibration analysis of beams or beam-like elements with different cross-sections.

Keywords: free vibration; transverse cracks; finite element: beam; ABAQUS.

1. Introduction

The widespread use of metallic components is realized under a variety of static and progressive dynamic loads during service. In this context, many engineering systems inevitably encounter structural defects, including cracks as a result of mechanical vibrations, critical environmental conditions, corrosion, extended service periods and cyclic loads, etc. The initiation of transverse cracks in key structural components poses an alarming consequence of reducing structural

functionality and, subsequently, the risk of catastrophic failure of the structure. The flexibility induced due to cracks modifies the dynamic conduct of the structural element as it reduces the stiffness of the beam, ultimately leading to failure. Thus, for structural safety, the investigation on crack behavior under dynamic conditions is a significant technical and scientific issue that requires a comprehensive research attention. In this context, research attempts were undertaken for compiling the related vibration-based analyses in order to understand and emphasize the significance of crack analysis for beams [1–3].

The shifting of vibration signatures under dynamic settings may be used to understand how structural abnormalities cause damages such as stiffness changes, structural deterioration, and fatigue characteristics [4]. When a fracture or a fault that resembles a crack is present, the problems with evaluating the vibration of beams become more complex. Yet, the problem remains of great interest since a robust and all-encompassing research effort to examine the frequency changes of fractured beams is seldom addressed and far from complete [5].

Researchers have calculated the natural frequencies of fractured Bernoulli-Euler beams with open fractures by solving boundary value problems and motion equations. A number of methods have been put forth for this purpose, including the formulation of equations to account for changes in natural frequencies brought on by cracks in beams [6], a Galerkin solution for symmetric double-edge mid-span cracks, derivation of natural frequencies for a damaged cantilever beam with single-edge and double-edge cracks, and more [7, 8]. The approaches for addressing vibration issues in damaged structures have been thoroughly studied, and a continuous cracked beam vibration theory for simply supported beams with single-edge and double-edge cracks has been devised and experimentally proven [9]. Heaviside and Dirac's delta distribution functions have been used in works to handle beam vibration issues with numerous open fractures and to derive dynamic stiffness matrices for cracked frames [10]. Researchers have employed rotating springs to depict single fractures or a reduction in stiffness along the damaged length to imitate cracks [11, 12]. The stiffness reduction is caused by changes in the material's cross-sectional area or Young's modulus. Additionally, the strain energy density function and fracture mechanics techniques have been used to experimentally develop the relationship between crack depth and equivalent spring stiffness.

Alshorbagy *et al.* [13] examined the dynamic characteristics of a functionally graded beam with the variation of material distribution axially or transversally through the depth of the beam. Soltani *et al.* [14] developed a numerical technique for free vibration and stability analysis of thin-walled beams with flexural–torsional coupling effect. Biswal *et al.* [15] presented a finite element analysis of a cracked beam using the Timoshenko beam theory and Hamilton's

principle while considering the effect of structural damping. Canales and Mantari [16] presented the vibrational behavior of isotropic and laminated beams using the Carrera unified solution and Ritz method. Lee and Lee [17] obtained a transfer matrix method to analyze the free vibration characteristics and eigenvalue analyses of a functionally graded beam. The matrix was derived from the correlation of displacement and forces at the beam ends. Corrêa et al. [18] examined the accuracy of the generalized or extended finite element approach for the free vibration analysis of curved beams. Yang et al. [19] proposed a CUF-1D method to accurately predict natural frequencies and dynamic response of thin-walled composite beams. Given the significance of cracks and crack-like structural discontinuities, a notable amount of research was addressed to damage analysis in structural elements for a spectrum of materials using different methods [20–24].

The research discussed above addresses the vibration of beam-like structures in the presence of cracks, providing a sound idea about the effects of cracks on natural frequencies. However, the existing literature mostly highlights the impact of a single crack on the natural frequency of the beam. The study of vibration in multi-cracked beam structures is not fully covered and remains incomplete. Furthermore, a systematic and in-depth analysis regarding multiple cracks presents a significant scientific research perspective. Thus, keeping these aspects in consideration, the present work is undertaken.

2. Mathematical modeling

The geometric dimensions – length (L), width (b) and thickness (h) – for an isotropic beam with a rectangular cross-section are shown in Fig. 1. The crack
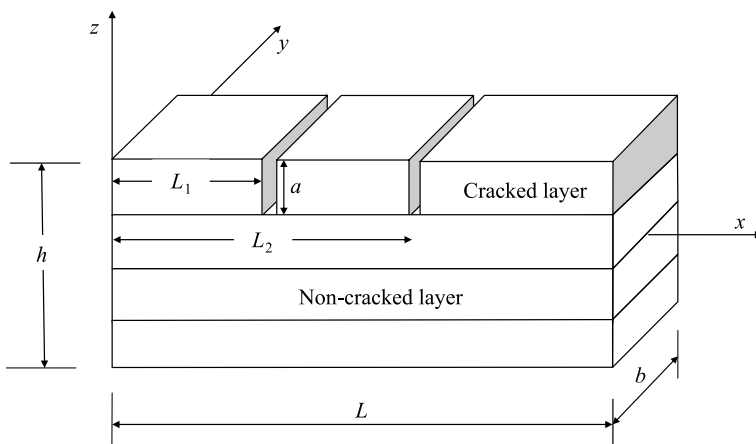

Fig. 1. Typical laminated composite cracked beam element with rectangular cross-section and co-ordinate axes.

positions are defined at L_1, L_2 from the left end and the depth of the transverse crack is denoted as a. The cracked beam model can be extended to multiple cracks located at $L_3, L_4, ..., L_i$. The intact beam finite element (FE) modeling is conducted in line with [9], whereas the cracked beam FE is modeled as below.

In the present analysis, the FE formulation is presented using an 8-noded isoparametric element from the ABAQUS library, using a brick element. Thus, considering this brick element, the displacement fields can be assumed based on the first-order shear deformation theory (FSDT) as per [25]:

$$(2.1) \qquad\qquad u(x,y,z) = u_0(x,y) + z\theta_x,$$

$$(2.2) \qquad\qquad v(x,y,z) = v_0(x,y) + z\theta_y,$$

$$(2.3) \qquad\qquad w(x,y,z) = w_0(x,y),$$

where the displacement components are u, v and w along the coordinate system x, y and z, respectively, u_0, v_0 and w_0 are the respective displacement components of the midplane section, and θ_x and θ_y denote rotations in the x-z and y-z planes, respectively.

The idea of analyzing the isotropic beam through a layer-wise model is adopted from previously addressed notable research works on the dynamics of layered beams [26–28]. Consenquently, the beam simulation model was developed layer-wise to facilitate the smooth assignment of transverse cracks. To study the effects of cracks on the natural frequencies, an infinitesimal element of the layer-wise composite beam (LCB) encompassing the cracked region is identified for study to govern the local compliance matrix adequately, as demonstrated in Fig. 1. Within this frame of reference, the local compliance matrix for the element is written as:

$$(2.4) \quad c_{ij} = \frac{\partial^2}{\partial P_i \partial P_j} \int\limits_A \left(D_1 \sum_{n=1}^{6} K_{\mathrm{I}n}^2 + D_2 \sum_{n=1}^{6} K_{\mathrm{II}n}^2 \right.$$

$$\left. + D_{12} \sum_{n=1}^{6} K_{\mathrm{I}i} \sum_{n=1}^{6} K_{\mathrm{II}n} + D_3 \sum_{n=1}^{6} K_{\mathrm{III}n}^2 \right) \mathrm{d}A,$$

where A is the cracked surface area and D_1, D_2, D_3, and D_{12} are the material parameters coefficients and expressed as:

$$D_1 = -0.5\bar{b}_{11}\mathrm{Im}\left(\frac{\mu_1 + \mu_2}{\mu_1\mu_2}\right), \qquad D_{12} = \bar{b}_{11}\mathrm{Im}\left(\mu_1\mu_2\right)K_{\mathrm{I}}K_{\mathrm{II}},$$

$$D_2 = 0.5\bar{b}_{11}\mathrm{Im}\left(\mu_1 + \mu_2\right), \qquad D_3 = 0.5\left(\bar{b}_{44}\bar{b}_{55}\right)^{1/2}.$$

The stress intensity factors K_{I}, K_{II}, and K_{III} are accounted for crack modes I, II, and III respectively [29], $\bar{b}_{ij}$ accounts for the local compliance of the composite material, and the characteristic equation roots are μ_1 and μ_2 [30].

The determination of the compliance matrix or flexibility matrix effectively and conveniently defines the stiffness matrix of the cracked beam. The total flexibility matrix is calculated by measuring the cracked and intact portions. In order to obtain the equivalent compliance coefficients to represent the stiffness matrix for the cracked element, the length and mass of cracked element are considered as zero [31]. An archetypal rectangular composite cracked beam element is illustrated in Fig. 1 and it is modeled by applying stress intensity factors in fracture mechanics. Using stress intensity factors, the cracked section local compliance matrix is written in line with [32]:

$$
(2.5) \qquad [C] =
\begin{bmatrix}
2D_1 & 1.5D_1 & 0 & 12\dfrac{D_1}{h} & 12\dfrac{D_1}{b} \\[2ex]
1.5D_1 & 4.5D_2 & 0 & 9\dfrac{D_{12}}{h} & 9\dfrac{D_{12}}{b} \\[2ex]
0 & 0 & 4.5D_3 & 0 & 0 \\[2ex]
12\dfrac{D_1}{h} & 9\dfrac{D_{12}}{h} & 0 & 72\dfrac{D_1}{h^2} & 36\dfrac{D_1}{bh} \\[2ex]
12\dfrac{D_1}{b} & 9\dfrac{D_{12}}{b} & 0 & 36\dfrac{D_1}{bh} & 96\dfrac{D_1}{b^2}
\end{bmatrix}
* \dfrac{\prod L_i^2}{bh^2},
$$

where L_i denotes crack location.

The crack simulation in ABAQUS follows the concept of inverting the local compliances to obtain the stiffness matrix of the cracked element and subsequently evaluating the stiffness of the cracked beam. KISA [31] conducted a crack modeling for a 2-noded three degrees of freedom (DOF), and the stiffness matrix is presented as the inverse of the compliance matrix as follows:

$$
(2.6) \qquad K_C =
\begin{bmatrix}
[C]^{-1} & -[C]^{-1} \\
-[C]^{-1} & [C]^{-1}
\end{bmatrix}_{(6\times 6)}.
$$

Now following KISA [31], the stiffness can be improvised. For example, by extending Eq. (2.2) to a 3-noded LCB with five degrees of freedom, the resulting stiffness matrix for the cracked element is given by:

$$
(2.7) \qquad [K_{\mathrm{crack}}] =
\begin{bmatrix}
[C^{-1}] & -[C^{-1}] & 0 \\
-[C^{-1}] & 2[C^{-1}] & -[C^{-1}] \\
0 & -[C^{-1}] & [C^{-1}]
\end{bmatrix}_{(15\times 15)}.
$$

During vibration simulation, the ABAQUS platform is capable of generating a very defined mesh divisions that essentially capture eigenfrequencies effectively, regardless of the total global DOFs in the system. Thus, the ABAQUS finite element suite presents an advantage to be used for modal simulation results.

The cracked laminated beam stiffness matrix is given by:

$$(2.8) \qquad [K_{cbe}] = [K_e] - [K_{\text{crack}}],$$

where $[K_{cbe}]$ is the stiffness of the cracked beam element, $[K_e]$ is the stiffness of the non-cracked beam element, and $[K_{\text{crack}}]$ is the stiffness of the cracked element.

The governing eigenvalue equation for LCB with a crack is

$$(2.9) \qquad \left([K] - \omega^2 [M]\right) \{\Delta\} = 0,$$

where $[K]$ is the cracked beam stiffness matrix, $[M]$ is the beam mass matrix, ω is the frequency, and $\{\Delta\}$ is the vector of degrees of freedom.

The mass matrix will not change due to the initiation of cracks. The mass matrix can be represented as:

$$(2.10) \qquad M_e = \int\limits_{-1}^{+1} \int\limits_{-1}^{+1} [N]^{\mathrm{T}} [P] [N] |J| \, \mathrm{d}\xi \, \mathrm{d}\eta,$$

where $[N]$ accounts for shape function, $[B]$ is referred to as the strain-displacement matrix, and $|J|$ is the Jacobian determinant.

The shape functions for an 8-noded isoparametric element are

$$N_i = \frac{1}{4} \left(\xi^2 + \xi\xi_i\right) \left(\eta^2 + \eta\eta_i\right), \qquad i = 1, 2, 3, 4,$$

$$N_i = \frac{1}{2} \left(1 - \xi^2\right) \left(\eta^2 + \eta\eta_i\right), \qquad i = 5, 7,$$

$$N_i = \frac{1}{2} \left(\xi^2 + \xi\xi_i\right) \left(1 - \eta^2\right), \qquad i = 6, 8,$$

and $[P]$ is known as the inertia matrix.

3. Simulation of finite element modeling using ABAQUS

A linear beam FE model is erected in the ABAQUS platform for recording simulation results. The pre-processing begins with developing the laminated

beam geometry and assigning elastic properties to each layer. After assigning material properties, assembling is performed and crack signatures are defined. The pre-processing step is followed by analysis, involving fixing boundary conditions, selecting suitable mesh size and simulating crack. The analysis is then followed by post-processing, where the modal analysis is performed and the simulated results for eigenfrequencies are recorded. Mode shapes and numerical modal frequencies from the ABAQUS platform are presented in Fig. 2.
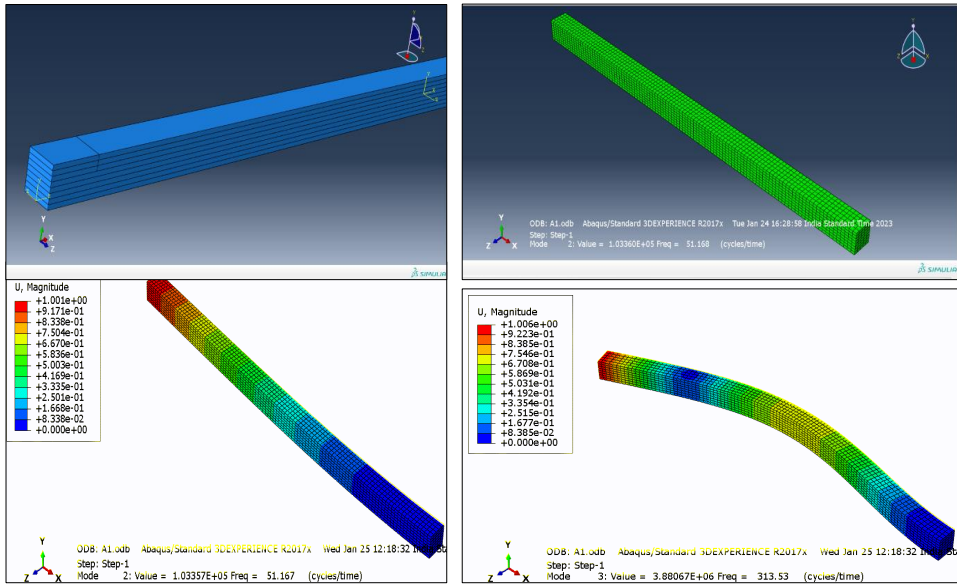
Fig. 2. Beam modelling and simulation using ABAQUS.

According to the ABAQUS documentation, using a well-structured mesh composed of hexahedral elements (C3D8R) often yields a solution of comparable accuracy while being more cost-effective. This is supported by insights observed in previous notable research work [33].

4. Results and discussions

The results of beam vibration frequencies are obtained from numerical analysis for an aluminum beam with transverse open cracks and presented with respect to different parameters. In view of the analysis, the results are categorized as follows:

- convergence study,
- comparison of present FE results with previous studies,
- simulated results for different parameters.

4.1. Convergence study

In order to facilitate a definite and suitable mesh division, the beam FE model is simulated in the ABAQUS platform for natural frequencies of vibration concerning different fiber orientations. In line with [16], the convergence study is performed, considering material type, geometry and elastic properties in equal measures and the same domain of analysis. The results are summarized in Table 1. From the convergence study, a mesh division of 4500 elements is reported to exhibit optimal results in comparison with [16]. Consequently, further vibration study in this research work is performed employing this mesh division consistently.

Table 1. The convergence of non-dimensional fundamental natural frequency ($\widetilde{\omega}$) of beam. $E = 100$ GPa, $\nu = 0.3$, $L/h = 10$ (clamped-clamped boundary condition), $\widetilde{\omega} = \frac{\omega L^2}{h}\sqrt{\frac{\rho}{E}}$.

Mesh division	Non-dimensional natural frequency ($\widetilde{\omega}$)
1000 elements	6.324
2000 elements	6.521
3000 elements	6.633
4000 elements	6.756
4500 elements	6.754
5000 elements	6.753
Ref. [16]	6.977

4.2. Comparison of present FE analysis with previous studies

The precision and proficiency of the present FE modeling through ABAQUS are validated with regard to previous studies. Vibration frequencies for a cracked cantilever beam, specifically for the relative crack depth (RCD), recorded through ABAQUS, are compared with those obtained from [34] in the same testing domain, using exact material parameters as in [34]. The results are summarized in Table 2. The present results demonstrate good agreement with those obtained in [34]. The geometry and material details are listed below.

Table 2. First natural frequency comparison for clamped-free beam with an open crack ($L_1/L = 0.25$ from clamped end).

Frequency mode	RCD	Ref. [34]		Present
		FEM	Spectral model	
	0.05	26.12	26.138	26.147
Fundamental frequency	0.25	25.83	26.075	25.94
	0.5	25.196	25.196	25.22

4.3. Simulated results

The simulated results for eigenfrequencies of a cracked beam for different boundary conditions are recorded on the ABAQUS platform. The boundary conditions are considered as clamped-free (CF), clamped-clamped (CC) and simply supported (SS). An aluminum beam is considered for the investigation with the following material properties $E = 70$ GPa, $G = 26$ GPa, Poisson's ratio $= 0.3$, and $\rho = 2700$ kg/m^3. The length of the beam is set to 750 mm, and the width and depth are both 35 mm.

4.3.1. Effect of CF boundary condition on the natural frequencies of a cracked beam. The beam simulation model, developed in ABAQUS, is inflicted with relative crack depth (RCD) of 0.25, 0.5, and 0.75 at relative crack positions (RCP) of 0.1, 0.3, 0.5, 0.7, and 0.9. For the crack effect analysis, each crack depth is increased at each RCP, and the results are graphically presented in Fig. 3. The figure illustrates the fundamental natural frequencies for the isotropic beam subjected to CF boundary condition at various relative crack positions for varying relative crack depths. It is observed in Fig. 3 that when the crack is positioned at $0.1L$, there is a significant decrease in the magnitude of natural frequencies with an increase in RCD. Furthermore, the gradual shifting of crack locations from the fixed end results in an increase in natural frequency, approaching the magnitude closer to the intact beam. Moreover at $0.9L$ crack position, changes in frequencies are insignificant compared to the frequency magnitude of the intact beam. It is observed that the change in natural frequency is maximum when the crack is at the fixed end and near the free end, the natural frequencies are nearly equal to those of the intact beam.
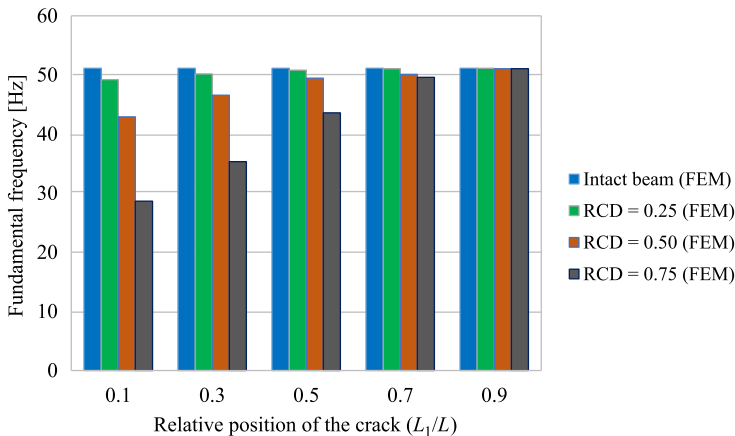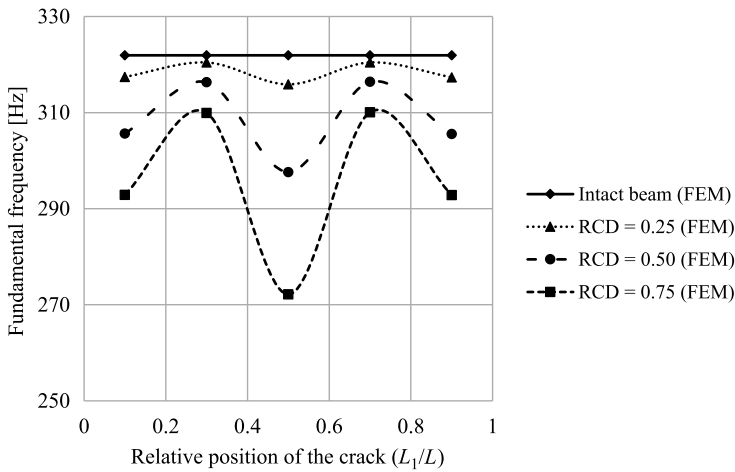

Fig. 3. Variation in fundamental frequency for CF beam concerning crack depth and location.

4.3.2. Effect of CC boundary condition on the natural frequencies of cracked beam. The effect of CC boundary condition on the natural frequency is presented graphically in Fig. 4. In this analysis, the RCD and RCP are considered as earlier for the CF beam. The depiction in Fig. 4 shows minimal changes in frequency magnitude when cracks are located at $0.1L$ and $0.9L$. Furthermore, at the crack position $0.3L$ and $0.7L$, no noticeable changes in frequencies are observed. Furthermore, the frequency magnitudes are more closely aligned with the intact beam. However, a significant decrement in the fundamental frequencies is observed at the $0.5L$ crack position. The maximum changes in the natural frequencies in the case of CC boundary condition occur at the center of the beam. This is attributed to the fact that the beam is restrained at both ends.

Fig. 4. Variation in fundamental frequency for CC beam concerning crack depth and location.

4.3.3. Effect of SS boundary condition on the natural frequencies of cracked beam. Figure 5 shows the summary of crack effects on natural frequencies, considering SS boundary condition. It is observed in Fig. 5 that the graphical curve follows the same trend as that of the CC beam. However, the magnitudes of frequencies lie between the frequency magnitudes of the CF and CC beams. The maximum reduction in frequencies is observed at the center of the beam. When the cracks are located at $0.1L$ and $0.9L$, the deviation in frequency values is very small compared to that of CC boundary condition. In addition, very small changes can be observed at the crack position $0.3L$ and $0.7L$.

4.3.4. Effect of crack position on the natural frequencies of a laminated beam. In order to study the effect of crack position on the natural frequencies
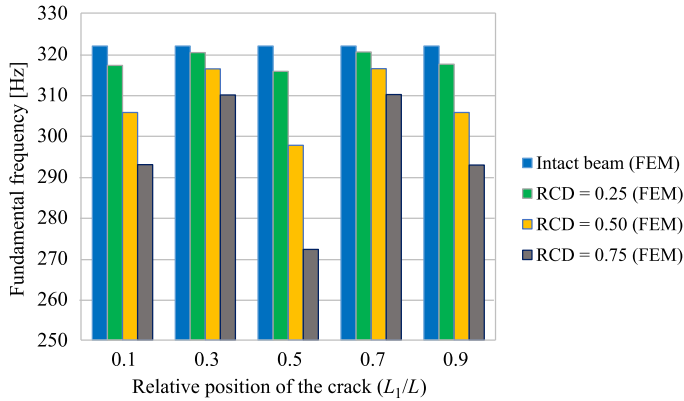
FIG. 5. Variation in fundamental frequency for SS beam concerning crack depth and location.

of the beam, crack locations at $0.1L$, $0.3L$, $0.5L$, $0.7L$, and $0.9L$ are considered. Fixed (CC) and cantilever (CF) support conditions are considered for this part of the analysis.

• *Effect of position of crack on CF beam for single crack on vibration.* The variations in vibration frequencies with respect to the position of a crack for the cantilever (CF) boundary condition are shown in Fig. 6. To analyze the single crack effect on natural frequencies, a relative crack depth of 0.375 is introduced at various locations. The FE simulation results for vibration frequencies, presented in Fig. 6, show that the maximum reduction in natural frequencies with respect to the intact beam is observed when the crack is located at $0.1L$ from the clamped edge. It is observed that the beam frequencies of vibration are least affected when cracks are positioned far from the clamped edges, as opposed to
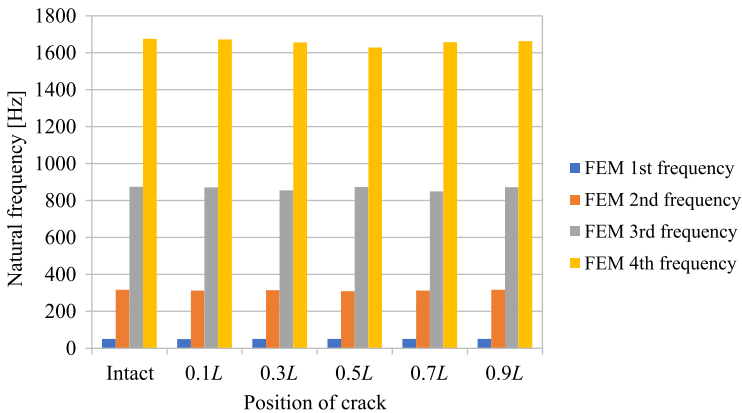

FIG. 6. Variation in vibration frequencies with respect to crack positions for CF beam with a single transverse crack and $a/h = 0.375$.

those located near the fixed end. Cracks near the free end exhibit almost equal frequencies of vibration as that of the intact beam. This observation agrees perfectly with the findings made by KISA and BRANDON [11], who employed a component mode synthesis analysis and FEM.

• *Effect of position of crack on CF beam for double crack under free vibration.* The variations in natural frequencies due to the position of two cracks for CF beam are shown in Fig. 7. Since previously it was found that the maximum reduction in natural frequency occurs at a position of $0.1L$, the analysis is conducted for the double crack, the crack is located constantly at $0.1L$, and the second crack is defined at $0.3L$, $0.5L$, $0.7L$, and $0.9L$ positions, respectively. The results presented in Fig. 7 show that the maximum reduction in vibration frequencies concerning two cracks occurs at locations $0.1L$ and $0.3L$ from the fixed end with respect to the non-cracked beam.
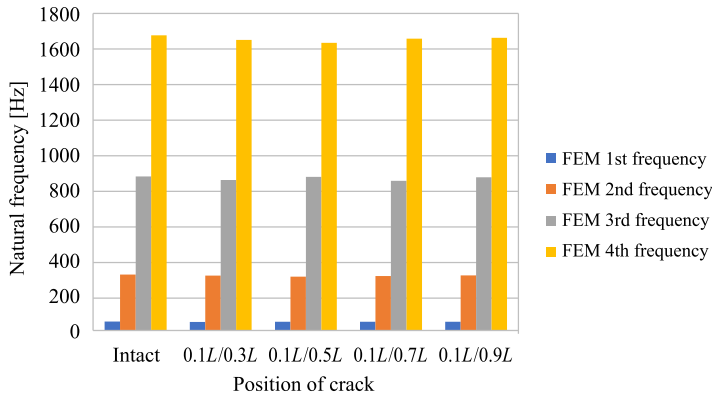

FIG. 7. Variation in vibration frequencies with respect to crack positions for CF beam with double transverse crack and $a/h = 0.375$.

• *Effect of position of crack on CF beam for triple crack under free vibration.* The variations in natural frequencies with respect to the position of three cracks are shown in Fig. 8 for the CF beam. Previously, it was found that the maximum reduction in natural frequency occurs at positions $0.1L$ and $0.3L$ and therefore two cracks are kept constant at crack location $0.1L$ and $0.2L$, while the third crack is defined at $0.5L$, $0.7L$, and $0.9L$, positions respectively. The results presented in Fig. 8 show that the maximum reduction in vibration frequencies concerning three cracks occurs at locations $0.1L$, $0.3L$, and $0.5L$ from the fixed end with respect to the non-cracked beam. Following this methodology, the multi-cracked beam may be analyzed for critical crack location and subsequently its severity can be assessed for structural functionality.
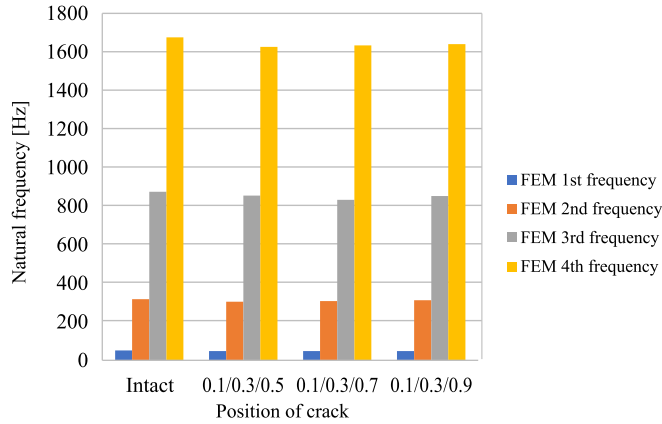
FIG. 8. Variation in vibration frequencies with respect to crack positions for CF beam with triple transverse crack and $a/h = 0.375$.

• *Effect of position of crack on CC beam for single crack under free vibration.* The computed results for the natural fundamental frequency of the beam with a single transverse crack concerning crack positions are presented in Fig. 9 for the fixed (CC) boundary condition. A crack depth of $0.375h$ is considered for analysis. Following the sequential analysis observed for the CF beam, in order to analyze the effect of single transverse crack, the locations under observations are $0.1L$, $0.3L$, $0.5L$, $0.7L$, and $0.9L$, respectively. It is noticed from Fig. 9 that the crack located at $0.5L$ from the fixed support results in a maximum reduction in all modes of the natural frequency with respect to the intact composite beam.
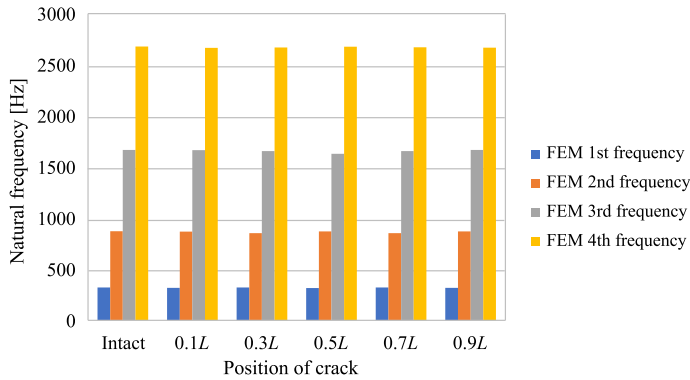

FIG. 9. Variation in vibration frequencies with respect to crack positions for CC beam with a single transverse crack and $a/h = 0.375$.

• *Effect of position of crack on CC beam for double crack under free vibration.* Figure 10 demonstrates the changes in natural frequencies due to the position
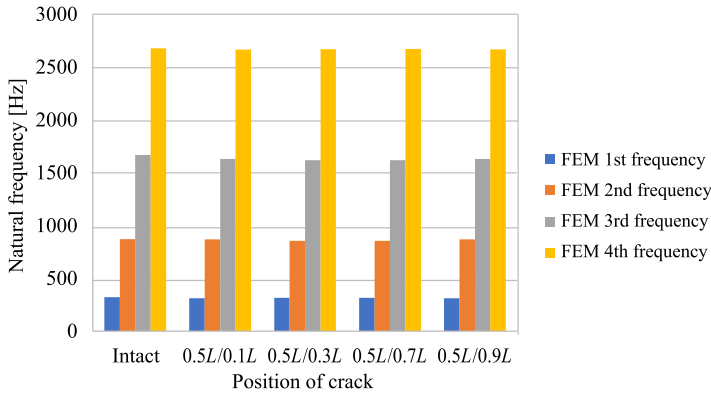
FIG. 10. Variation in frequencies of vibration with respect to crack positions for CC beam with two transverse cracks and $a/h = 0.375$.

of a double crack for CC boundary condition. For the analysis of the double crack, the crack location at $0.5L$ is kept constant, as it results in a maximum reduction in frequencies of vibration for a single crack. The second crack is varied at $0.1L$, $0.3L$, $0.7L$, and $0.9L$ positions, respectively. In this case, the maximum reduction in vibration frequencies of LCB is observed at locations $0.1L$, $0.5L$ from the clamped support.

4.3.5. Effect of crack depth on the natural frequencies of laminated beam. To analyze the effects of crack depth on natural vibration frequencies, five definite RCDs $a/h = 0$, 0.125, 0.25, 0.375, 0.5, 0.625, and 0.75 are explored. For this segment of the analysis, fixed (CC) and cantilever (CF) boundary conditions are considered.

• *Effect of depth of crack on CF beam under free vibration.* The variations in the beam vibration frequency with respect to RCD are presented in Figs. 11–13 for the aluminum beam with implications of a single, double, and triple crack, respectively. The frequency measurements are done for the CF beam under free vibration. It is found that for CF beams, the critical locations are $0.1L$ for a single crack, $0.1L$, $0.3L$ for two cracks, and $0.1L$, $0.3L$ and $0.5L$ for three cracks. For each case, the RCDs are varied from 0 to 0.75. It is noticed from Figs. 11–13 that up to an RCD of 0.5, the changes in frequency are insignificant, whereas a considerable reduction in natural frequencies is observed for an RCD greater than 0.5. A definite outcome is noticed from the figures that the vibration frequencies do not change significantly when the crack is located at the far end, and then gradually shifts towards the fixed end, variations are observed in natural frequencies. This phenomenon occurs because of the maximum bending moment at the fixed end. The variations in fundamental frequency are very small
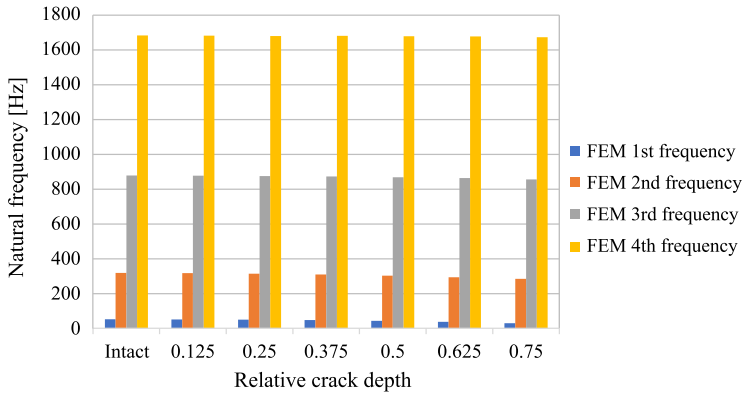
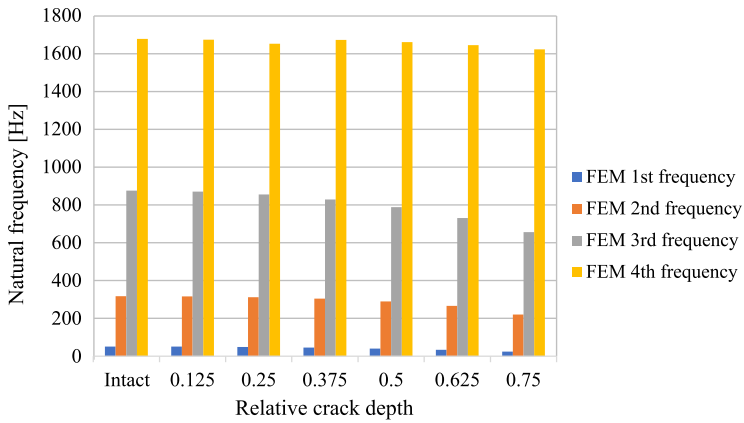FIG. 11. Effect of RCD for cantilever beam with a single crack.

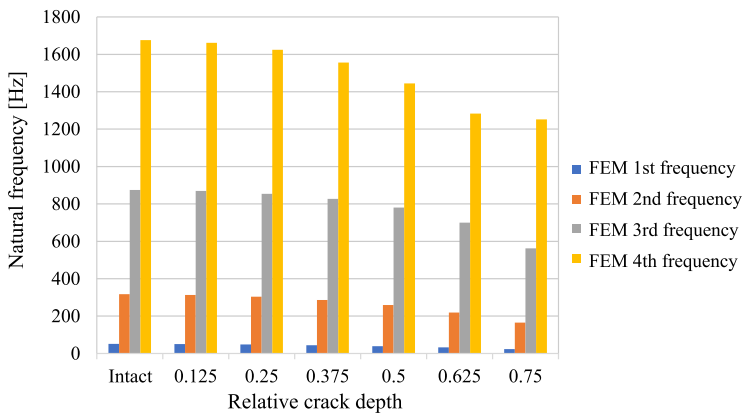FIG. 12. Effect of RCD for cantilever beam with a double crack.

FIG. 13. Effect of RCD for cantilever beam with a triple crack.

or negligible compared to that of a non-cracked beam due to a crack at the free end because of the least bending moment in that region. Also, it may be noted that there are reduced vibration frequencies as the crack depth increases for any particular location.

• *Effect of depth of crack on CC beam under free vibration.* The changes in the beam natural frequencies concerning the RCDs under the clamped condition at both ends are shown in Figs. 14–16. The recorded single, double, and triple crack results are summarized in these graphs, respectively. The analysis procedure follows a similar trend as observed for the CF case. It is noticed from graphical summarizations that for an RCD of 0.125 to 0.375, the fundamental frequency variation is insignificant, whereas from a crack depth of $0.5h$ onwards, the frequency falls quite significantly compared to the intact beam. The higher mode frequencies also exhibit a similar pattern where the variations in natural
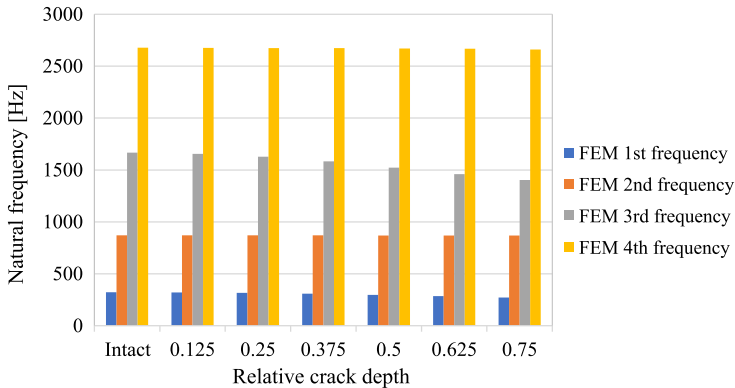

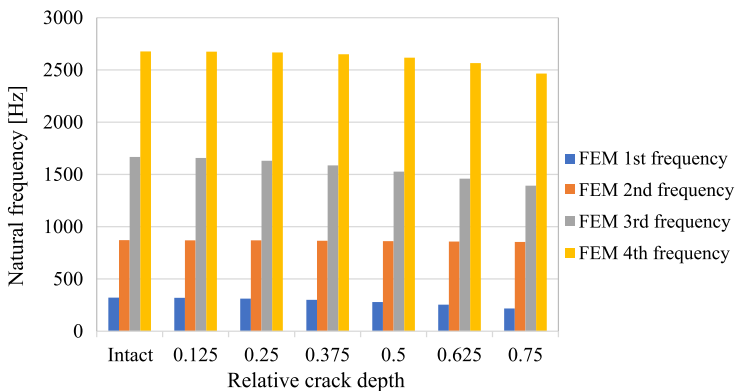FIG. 14. Effect of relative crack depth for clamped beam with single crack.

FIG. 15. Effect of relative crack depth for clamped beam with double crack.
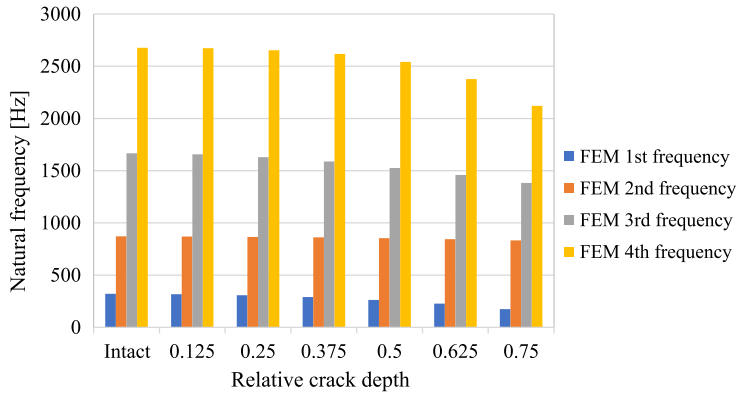
Fig. 16. Effect of relative crack depth for clamped beam with triple crack.

frequencies for crack depths $0.125h$ to $0.375h$ are insignificant, but with increasing crack depth, a considerable reduction in frequencies of vibration is recorded. It indicates that the increased crack number severely affects the natural frequency and noticeably decreases the beam vibration frequencies for an RCD higher than 0.5.

5. Conclusion

In this study, the frequency-based analysis was conducted for a cracked isotropic beam to examine the variations in beam frequencies with respect to different beam parameters. The ABAQUS software, based on FEM, was employed for numerical computation. The following conclusions are drawn from the presented results:

- The beam simulation model developed in the ABAQUS platform can provide consistent modal frequencies for all modes of interest, providing information on the crack effects on vibration frequencies.
- The convergence data obtained from numerical simulations further indicates that a fine mesh division is essential in capturing the impact of cracks on modal frequencies. Additionally, a fine-mesh division can effectively produce the modal simulation results, regardless of the total degrees of freedom in the global system. This is an advantage of using a FE suite such as ABAQUS.
- Significant variations in vibration frequencies are observed for greater crack depth.
- Cracks located near the clamped support exhibit the maximum reduction in natural frequency for any particular crack depth.

- Frequencies decrease with an increase in relative crack depth.
- The CF beam exhibits lower magnitude in natural frequency compared to other boundary conditions, while the CC beam exhibits greater natural frequency.

References

1. MORENO-GARCÍA P., ARAÚJO DOS SANTOS J.V., LOPES H., A review and study on Ritz method admissible functions with emphasis on buckling and free vibration of isotropic and anisotropic beams and plates, *Archives of Computational Methods in Engineering*, **25**(3): 785–815, 2018, doi: 10.1007/s11831-017-9214-7.

2. GAYEN D., TIWARI R., CHAKRABORTY D., Static and dynamic analyses of cracked functionally graded structural components: a review, *Composites Part B: Engineering*, **173**: 106982, 2019, doi: 10.1016/j.compositesb.2019.106982.

3. SINHA G.P., KUMAR B., Review on vibration analysis of functionally graded material structural components with cracks, *Journal of Vibration Engineering & Technologies*, **9**: 23–49, 2021, doi: 10.1007/s42417-020-00208-3.

4. PENG Z.K., LANG Z.Q., CHU F.L., Numerical analysis of cracked beams using nonlinear output frequency response functions, *Computers & Structures*, **86**(17–18): 1809–1818, 2008, doi: 10.1016/j.compstruc.2008.01.011.

5. MATBULY M.S., RAGB O., NASSAR M., Natural frequencies of a functionally graded cracked beam using the differential quadrature method, *Applied Mathematics and Computation*, **215**(6): 2307–2316, 2009, doi: 10.1016/j.amc.2009.08.026.

6. CADDEMI S., MORASSI A., Multi-cracked Euler–Bernoulli beams: Mathematical modeling and exact solutions, *International Journal of Solids and Structures*, **50**(6): 944–956, 2013, doi: 10.1016/j.amc.2009.08.026.

7. OSTACHOWICZ W.M., KRAWCZUK M., Analysis of the effect of cracks on the natural frequencies of a cantilever beam, *Journal of Sound and Vibration*, **150**(2): 191–201, 1991, doi: 10.1016/0022-460X(91)90615-Q.

8. BAKHTIARI-NEJAD F., KHORRAM A., REZAEIAN M., Analytical estimation of natural frequencies and mode shapes of a beam having two cracks, *International Journal of Mechanical Sciences*, **78**: 193–202, 2014, doi: 10.1016/j.ijmecsci.2013.10.007.

9. CHONDROS T.G., DIMAROGONAS A.D., YAO J., Vibration of a beam with a breathing crack, *Journal of Sound and Vibration*, **239**(1): 57–67, 2001, doi: 10.1006/jsvi.2000.3156.

10. CADDEMI S., CALIÒ I., Exact closed-form solution for the vibration modes of the Euler–Bernoulli beam with multiple open cracks, *Journal of Sound and Vibration*, **327**(3–5): 473–489, 2009, doi: 10.1016/j.jsv.2009.07.008.

11. KISA M., BRANDON J., The effects of closure of cracks on the dynamics of a cracked cantilever beam, *Journal of Sound and Vibration*, **238**(1): 1–18, 2000, doi: 10.1006/jsvi.2000.3099.

12. ALTUNIŞIK A.C., OKUR F.Y., KARACA S., KAHYA V., Vibration-based damage detection in beam structures with multiple cracks: modal curvature vs. modal flexibility methods, *Non-destructive Testing and Evaluation*, **34**(1): 33–53, 2019, doi: 10.1080/1058 9759.2018.1518445.

13. ALSHORBAGY A.E., ELTAHER M.A., MAHMOUD F., Free vibration characteristics of a functionally graded beam by finite element method, *Applied Mathematical Modelling*, **35**(1): 412–425, 2011, doi: 10.1016/j.apm.2010.07.006.

14. SOLTANI M., ASGARIAN B., MOHRI F., Elastic instability and free vibration analyses of tapered thin-walled beams by the power series method, *Journal of Constructional Steel Research*, **96**: 106–126, 2014, doi: 10.1016/j.jcsr.2013.11.001.

15. BISWAL A.R., ROY T., BEHERA R.K., PRADHAN S.K., PARIDA P.K., Finite element based vibration analysis of a nonprismatic Timoshenko beam with transverse open crack, *Procedia Engineering*, **144**: 226–233, 2016, doi: 10.1016/j.proeng.2016.05.028.

16. CANALES F.G., MANTARI J.L., Free vibration of thick isotropic and laminated beams with arbitrary boundary conditions via unified formulation and Ritz method, *Applied Mathematical Modelling*, **61**: 693–708, 2018, doi: 10.1016/j.apm.2018.05.005.

17. LEE J.W., LEE J.Y., Free vibration analysis of functionally graded Bernoulli-Euler beams using an exact transfer matrix expression, *International Journal of Mechanical Sciences*, **122**: 1–17, 2017, doi: 10.1016/j.ijmecsci.2017.01.011.

18. CORRÊA R.M., ARNDT M., MACHADO R.D., Free in-plane vibration analysis of curved beams by the generalized/extended finite element method, *European Journal of Mechanics – A/Solids*, **88**: 104244, 2021, doi: 10.1016/j.euromechsol.2021.104244.

19. YANG H., DANESHKHAH E., AUGELLO R., XU X., CARRERA E., Numerical vibration correlation technique for thin-walled composite beams under compression based on accurate refined finite element, *Composite Structures*, **280**: 114861, 2022, doi: 10.1016/j.compstruct.2021.114861.

20. DARPE A.K., GUPTA K., CHAWLA A., Coupled bending, longitudinal and torsional vibrations of a cracked rotor, *Journal of Sound and Vibration*, **269**(1–2): 33–60, 2004, doi: 10.1016/S0022-460X(03)00003-8.

21. SEKHAR A.S., Multiple cracks effects and identification, *Mechanical Systems and Signal Processing*, **22**(4): 845–878, 2008, doi: 10.1016/j.ymssp.2007.11.008.

22. JASSIM Z.A., ALI N.N., MUSTAPHA F., ABDUL JALIL N.A., A review on the vibration analysis for a damage occurrence of a cantilever beam, *Engineering Failure Analysis*, **31**: 442–461, 2013, doi: 10.1016/j.engfailanal.2013.02.016.

23. JAIN A.K., RASTOGI V., AGRAWAL A.K., Experimental investigation of vibration analysis of multi-crack rotor shaft, *Procedia Engineering*, **144**: 1451–1458, 2016, doi: 10.1016/j.proeng.2016.05.177.

24. SENTHILKUMAR M., MANIKANTA REDDY S., SREEKANTH T.G., Dynamic study and detection of edge crack in composite laminates using vibration parameters, *Transactions of the Indian Institute of Metals*, **75**(2): 361–370, 2022, doi: 10.1007/s12666-021-02419-y.

25. SAHU S.K., DAS P., Experimental and numerical studies on vibration of laminated composite beam with transverse multiple cracks, *Mechanical Systems and Signal Processing*, **135**: 106398, 2020, doi: 10.1016/j.ymssp.2019.106398.

26. PROKUDIN O.A., SOLYAEV Y.O., BABAYTSEV A.V., ARTEMYEV A.V., KOROBKOV M.A., Dynamic characteristics of three-layer beams with load-bearing layers made of alumino-glass plastic, *PNRPU Mechanics Bulletin*, **2020**(4): 260–270, 2020, doi: 10.15593/perm.mech/2020.4.22.

27. KRYSKO A.V., AWREJCEWICZ J., SALTYKOVA O.A., ZHIGALOV M.V., KRYSKO V.A., Investigations of chaotic dynamics of multi-layer beams taking into account rotational inertial effects, *Communications in Nonlinear Science and Numerical Simulation*, **19**(8): 2568–2589, 2014, doi: 10.1016/j.cnsns.2013.12.013.

28. LEWANDOWSKI R., WIELENTEJCZYK P., LITEWKA P., Dynamic characteristics of multi-layered, viscoelastic beams using the refined zig-zag theory, *Composite Structures*, **259**: 113212, 2021, doi: 10.1016/j.compstruct.2020.113212.

29. TADA H., PARIS P.C., IRWIN G.R., *The Stress Analysis of Cracks. Handbook*, 3rd ed., Del Research Corporation, ASME Press, USA, 1973.

30. KRAWCZUK M., OSTACHOWICZ W.M., Modelling and vibration analysis of a cantilever composite beam with a transverse open crack, *Journal of Sound and Vibration*, **183**(1): 69–89, 1995, doi: 10.1006/jsvi.1995.0239.

31. KISA M., Free vibration analysis of a cantilever composite beam with multiple cracks, *Composites Science and Technology*, **64**(9): 1391–1402, 2004, doi: 10.1016/j.compscitech.2003.11.002.

32. NIKPUR K., DIMAROGONAS A., Local compliance of composite cracked bodies, *Composites Science and Technology*, **32**(3): 209–223, 1988, doi: 10.1016/0266-3538(88)90021-8.

33. YARDIMOGLU B., A novel finite element model for vibration analysis of rotating tapered Timoshenko beam of equal strength, *Finite Element in Analysis and Design*, **46**(10): 838–842, 2010, doi: 10.1016/j.finel.2010.05.003.

34. KRAWCZUK M., PALACZ M., OSTACHOWICZ W., The dynamic analysis of a cracked Timoshenko beam by the spectral element method, *Journal of Sound and Vibration*, **264**(5): 1139–1153, 2003, doi: 10.1016/S0022-460X(02)01387-1.